

Lift-off Stability of Hydrocarbon Jet Diffusion Flames

Fumiaki Takahashi

*National Center for Space Exploration Research on Fluids and Combustion
NASA Glenn Research Center
Cleveland, OH 44135, U.S.A.*

Viswanath R. Katta

*Innovative Scientific Solutions, Inc.
Dayton, OH, 45440, U.S.A.*

Abstract

The structure and stability of jet diffusion flames of gaseous hydrocarbon fuels in coflowing air at normal earth gravity have been investigated experimentally and computationally. Measurements of the critical mean jet velocity of methane, ethane, or propane at lifting or blowoff were made as a function of the co-flowing air velocity. Computations with 33 species and 112 elementary steps revealed the internal structures of the stabilizing region of methane and propane flames. The simulated flame base moved downstream under flow conditions close to the measured stability limit. A peak reactivity spot (i.e., reaction kernel) formed in the stabilizing region is responsible for the flame attachment and detachment processes.

INTRODUCTION

Diffusion flames are commonly used for industrial burners in furnaces and flares. Oxygen/fuel burners are usually diffusion burners, primarily for safety reasons, to prevent flashback and explosion in a potentially dangerous system. Furthermore, in most fires, condensed materials pyrolyze, vaporize, and burn in air as diffusion flames. As a result of the interaction of a diffusion flame with burner or condensed-fuel surfaces, a small quenched space is formed, thus leaving a diffusion flame edge, which plays an important role in flame holding in combustion systems and fire spread through condensed fuels. Despite a long history of jet diffusion flame studies, lifting/blowoff mechanisms have not yet been fully understood, compared to those of premixed flames.

By using a comprehensive computational fluid dynamics code [1] with detailed chemistry models, the authors [2-4] have numerically simulated the chemical-kinetic structure, the flame stability limit, and the propagation speed of edge diffusion flames in both fuel jets and flat-plate boundary layer. Major findings include that a peak reactivity spot, i.e., *reaction kernel*, is formed in the edge diffusion flame due to back-diffusion of radical species against an oxygen-rich incoming flow. Furthermore, heuristic linear correlations have been found between the reactivity (the heat-release or oxygen-consumption rate) and the velocity at the reaction kernel. This paper extends this effort using methane, ethane, and propane as the fuel.

EXPERIMENTAL PROCEDURE

The coaxial burner consists of a circular stainless-steel fuel tube (2.87 mm i.d.) placed vertically in a quartz chimney (85 mm i.d.) with co-flowing air in a vented combustion chamber

* Proceedings of the 20th International Colloquium on the Dynamics of Explosions and Reactive Systems (ICDERS), Montreal, Canada, July 31 – August 5, 2005

(255 mm i.d. \times 533 mm height). To provide uniform flow, two layers of honeycomb plates (1.6 mm cell size, 15 mm thickness, aluminum alloy) and two screens (40 mesh and 100 mesh, stainless steel) atop the honeycomb are placed in the base of the chimney. The flow rates of the fuel and air (house compressed air [filtered and dried]) are measured by calibrated mass flow meters. To determine the stability limit, the fuel flow rate is increased gradually at a fixed co-flowing air flow rate until flame liftoff or blowoff is observed. Two color video cameras capture the behavior of the flame and their S-video signals are recorded using DVCAM digital video cassette recorders.

NUMERICAL METHOD

The numerical code (UNICORN) developed by Katta et al. [1] solves time-dependent axisymmetric governing equations. The body-force term due to gravity is included in the axial-momentum equation. The momentum equations are integrated using an implicit QUICKEST numerical scheme for the convection terms, which is third-order accurate in both space and time and has a very low numerical-diffusion error. The finite-difference form of the species and enthalpy is obtained using the hybrid scheme with upwind and central differences.

The enthalpy of each species is calculated from polynomial curve-fits. Viscosity, conductivity, and diffusivity are estimated using molecular dynamics. Mixture viscosity and thermal conductivity are then estimated using the Wilke and Kee expressions [5], respectively. The effective diffusion coefficient of each species in the mixture is estimated using the binary diffusion coefficients and a mixture rule [5]. A C_3 -chemistry model [6] used for all fuels consists of 33 species and 112 elementary steps. The rate of the reaction $CH_3 + H + M \rightarrow CH_4 + M$ was found to be very sensitive to the subject phenomena and changed to that of Warnatz [7], since it yielded better agreement with existing experimental data for both counterflow diffusion flame extinction [8] and co-flow jet diffusion flame blow-off [2]. A optically thin-media broadband radiation heat-loss model [9] from CO_2 , H_2O , CH_4 , and CO was used.

The computational domain of 60×50 mm in the axial (z) \times radial (r) directions is represented by a mesh of 481×201 with clustered grid lines near the axisymmetric jet exit and a minimum spacing of 0.05 mm. The inner diameter and lip thickness of the fuel tube used for computations are $d = 2.88$ mm and 0.16 mm, respectively. The tube wall is assumed to be at a constant temperature (500 K). The fuel tube exit plane is placed 10 mm downstream from the inflow boundary in the open computational domain. Flat velocity profiles are prescribed for the fuel flow inside the tube and the air flow outside the tube as the inflow boundary conditions. The initial and boundary conditions for the axial (U) and radial (V) velocities and species and energy at different flow boundaries are the same as in previous work [2-4]. The fuel is methane or propane. The results reported in this paper were obtained for the mean fuel jet velocity (U_j) of 0.12 m/s and various mean air velocities (U_a) between 0.001 and 1.1 m/s.

RESULTS AND DISCUSSION

Figure 1 shows the measured stability limits; the critical mean jet velocity at the stability limit ($U_{j,c}$) decreased as the mean co-flowing air velocity was increased. The stability curves for methane and propane exhibit three regions: laminar branch, turbulent branch, and transition between them. The switching between the laminar and turbulent branches seems to be affected by the pipe flow transition as indicated by the critical Reynolds number ($Re = 2300$) in Fig. 1. For ethane, the transition did not occur in $U_a < 1.4$ m/s. At $U_a > 0.8$ m/s, the flame blew off

without forming a secondary stabilization point (lifted flame) as was reported previously [2], because the fuel jet at very low flow rates can easily be diluted excessively by the relatively fast coflowing air.

Figure 2 shows the calculated structure of a methane flame in a quasi-quiescent air environment, including the velocity vectors (\mathbf{v}), isotherms (T), total heat-release rate (q), local equivalence ratio (ϕ_{local}) on the right, the total molar flux vectors of atomic hydrogen (\mathbf{M}_H), oxygen mole fraction (X_{O_2}), oxygen consumption rate ($-\hat{\omega}_{O_2}$), and stoichiometric mixture fraction ($\xi_{\text{st}} = 0.055$) on the left. The local equivalence ratio, defined by considering a stoichiometric expression for intermediate species in the mixture to be converted to CO_2

and H_2O , is identical to the conventional equivalence ratio (ϕ) in the unburned fuel-air mixture. The mixture fraction was determined by the element mass fractions of carbon, hydrogen, and oxygen as defined by Bilger. The heat-release rate and the oxygen-consumption rate contours show the peak reactivity spot (reaction kernel) at the flame base. The heat-release rate and the oxygen-consumption rate contours show the peak reactivity spot (reaction kernel) at the flame base. The values at the fuel-lean reaction kernel were $q_k = 154 \text{ J/cm}^3\text{s}$, $-\hat{\omega}_{O_2,k} = 0.000472 \text{ mol/cm}^3\text{s}$, $|v_k| = 0.281 \text{ m/s}$, $T_k = 1545 \text{ K}$, $X_{O_2,k} = 0.036$, $\phi_{\text{local},k} = 0.71$, and $\xi_k = 0.052$.

Figure 3 shows the calculated structure of a methane flame at a near-lifting condition. The reaction kernel shifted 2.5 mm downstream from the jet exit, expanded the quenched zone, where more partial premixing occurred, and thus broadened radially. The longitudinal acceleration in the hot zone due to buoyancy made the velocity distributions more uniform downstream. The values at the reaction kernel were $q_k = 510 \text{ J/cm}^3\text{s}$, $-\hat{\omega}_{O_2,k} = 0.00155 \text{ mol/cm}^3\text{s}$, $|v_k| = 0.934 \text{ m/s}$, $T_k = 1567 \text{ K}$, $X_{O_2,k} = 0.057$, $\phi_{\text{local},k} = 0.77$, and $\xi_k = 0.051$. The reactivity and the velocity increased more than three times at the reaction kernel compared to those of the attached flame (Fig. 4), while the temperature remained nearly the same.

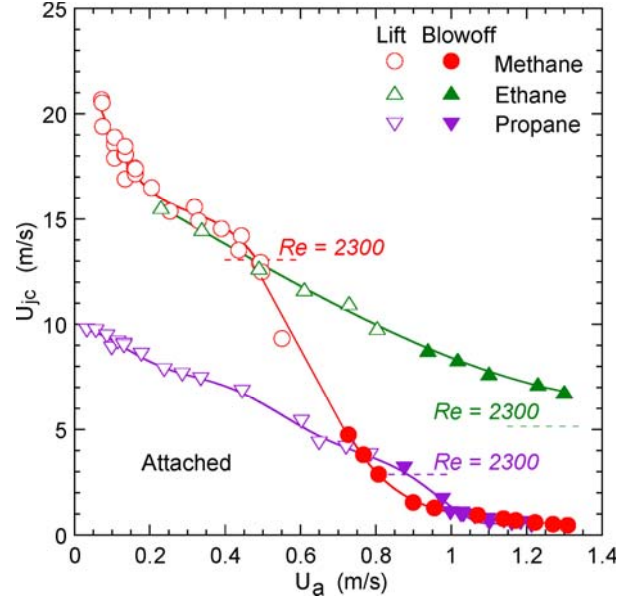


Fig. 1 Stability limits of co-flowing jet diffusion flames.

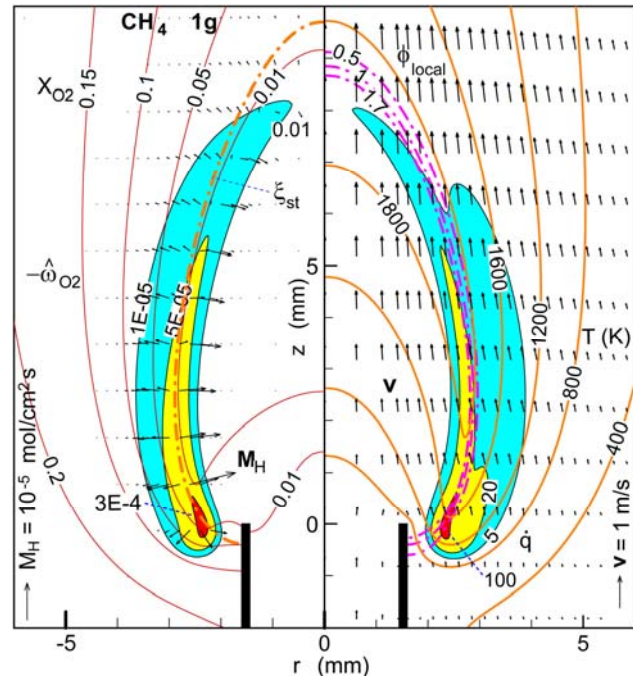


Fig. 2 Calculated structure of a methane jet diffusion flame. $U_j = 0.12 \text{ m/s}$; $U_a = 0.001 \text{ m/s}$.

CONCLUSIONS

The lifting limits of methane jet diffusion flames in coflowing air have been measured in normal earth gravity. Further numerical simulations of laminar jet diffusion flames in normal gravity using a C_3 -chemistry model extended linear correlations between the heat-release or oxygen-consumption rate and the velocity at the reaction kernel (a peak reactivity spot) in the flame base for methane and propane. The reaction kernel sustains stationary combustion in the incoming flow, by realizing a subtle balance between the overall reaction time and the residence time available, and thus holds the trailing diffusion flame. As the coflowing air velocity was increased, the reaction kernel was pushed inwardly and downstream, while increasing its reactivity by a blowing effect with an increased incoming velocity. As the standoff distance increased in the methane flame, the reaction kernel broadened radially and the slopes of reaction kernel correlations somewhat decreased toward lift-off.

ACKNOWLEDGMENT

This work was supported by the Office of Biological and Physical Research, National Aeronautics and Space Administration, Washington, DC. Assistance by Philip Werk, Benjamin Chan, and Jeffrey Taggart (CWRU) in conducting the experiment is acknowledged.

REFERENCES

1. Katta, V. R., Goss, L. P., and Roquemore, W. M., *AIAA J.* 32 (1994) 84.
2. Takahashi, F., and Katta, V. R., *Proc. Combustion Institute*, Vol. 28, 2000, pp. 2071-2078.
3. Takahashi, F., and Katta, V. R., *Proc. Combustion Institute*, Vol. 29, 2002, pp. 2509-2518.
4. Takahashi, F., and Katta, V. R., *Proc. Combustion Institute*, Vol. 30, 2004, in press.
5. Hirschfelder, J. O., Curtis, C. F., and Bird, R. B., *The Molecular Theory of Gases and Liquids*, Wiley, New York, 1954.
6. N. Peters, in: N. Peters and B. Rogg (Eds.), *Reduced Kinetic Mechanisms for Applications in Combustion Systems*. Springer-Verlag, Berlin, 1993, p. 3.
7. J. Warnatz, in: W. C. Gardiner (Ed.), *Combustion Chemistry*. Springer-Verlag, New York, 1984, p. 197.
8. Katta, V.R. and Roquemore, W.M., Central States Section Meeting/The Combustion Institute, 1996, pp. 449-454.
9. Annon., Computational Submodels, International Workshop on Measurement and Computation of Turbulent Nonpremixed Flames., <http://www.ca.sandia.gov/TNF/radiation.html>, 2003.

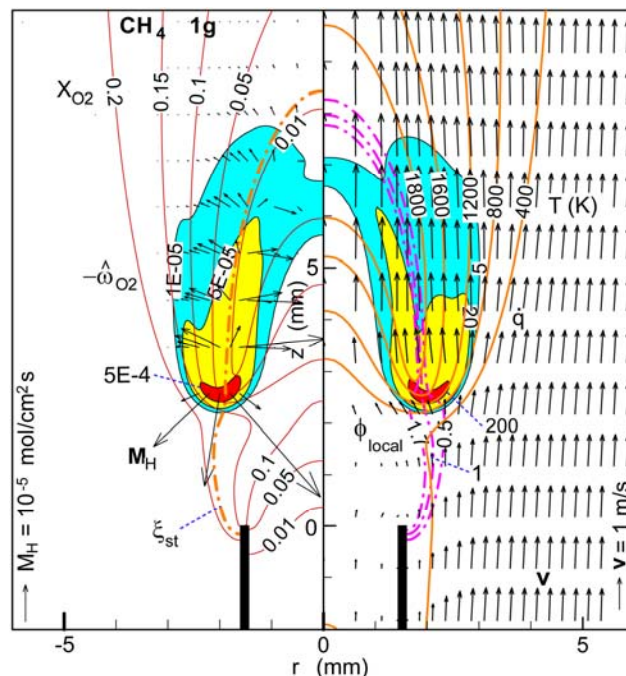


Fig. 3 Calculated structure of a methane jet diffusion flame. $U_j = 0.12$ m/s; $U_a = 1$ m/s